Dedicated Smart IR Barrier for Obstacle Detection in Railways

Juan J. García, Cristina Losada, Felipe Espinosa, Jesús Ureña, Álvaro Hernández, Manuel Mazo, Carlos de Marziani, Ana Jiménez, Emilio Bueno

Department of Electronics. University of Alcalá
Alcalá de Henares. Madrid. SPAIN
jesus@depeca.uah.es

Fernando Álvarez

Department of Electronics and Electromechanical Engineering. University of Extremadura. Cáceres. SPAIN

***Abstract* – This work presents an intelligent system, which allows to detect obstacles in railways, based on optical emitters. The sensorial system is based on a barrier of emitters and another of receivers, placed each one of them at one side of the railway. Apart from the disposition of the sensorial system, a codification method of the emission is also presented in order to detect the reception or the non-reception of transmissions between an emitter and a receiver. Obstacle detection is carried out by the lack of the reception in the detectors. A solution is proposed to reduce the number of false alarms related to these systems, by taking advantage of the high redundancy in the measurements. A high reliability under adverse conditions is achieved with the developed system, being possible to detect the presence of obstacles, and to inform about their position.**

I. INTRODUCTION

In the current railway systems, it is becoming more necessary to have safety elements in order to avoid accidents.

In this work, one of the causes, that can provoke serious accidents, is analysed: the existence in railways of obstacles, either fixed or mobiles. In railways, there are areas where an obstacle can likely appear, as overpasses with roads, or railway crossings. In the high-speed lines, zones close to overpasses are quite critical, since obstacles can fall. This can be caused by landslides, or simply by the fall of a vehicle or the transported material. The problem of landslides can also happen at entrances and exits of tunnels. In these critical areas, systems are usually located to detect the presence of obstacles [1][2], so they can inform about it to the control system. In this way, the train circulation can be stalled, and possible accidents are avoided.

In non high-speed lines (standard lines) there are other critical areas where it is necessary to detect the presence of obstacles: the level crossings. There are a lot of dedicated sensorial systems [3] installed in the level crossing area to avoid collision between trains and automobiles, captured on the railway when the crossing gates have started down.

These systems usually present the problem of generating false alarms, generating economical losses if the presence of obstacle is indicated, without this one should exist.

Regarding to these problems, the following aspects are analysed in this work: the sensorial system to use, and its geometric disposition; the emission codification of the selected sensor to provide the system with a high immunity to noise; false alarms discrimination and obstacle location.

II.SENSORIAL SYSTEM AND GEOMETRICAL DISTRIBUTION

Different references in literature deal about what type of sensorial system to use for the detection of obstacles in railways [1][2][4]. From the point of view of the weather conditions, a system radar [5] would be the most immune, but it presents a drawback with the detection of small obstacles on the line.

Cameras could also be used to control the areas of risk [3] [6], but the weather conditions (fog, hard rain, etc) and the economic aspects can discard their usage.

On the other hand, for the application described in the previous section, the trend is the use of optical sensors, either infrared or laser [1]. No matter the sensor type chosen, all the details, that will be discussed next, can be applied to both types. The selection between one of them will depend strongly on economic aspects. In this case, the shown results will be obtained using infrared emitters.

Infrared barriers usually consist of emitter-receiver pairs, located each one at a different side of the line, so it is only possible to detect the presence of an obstacle, but not its position.

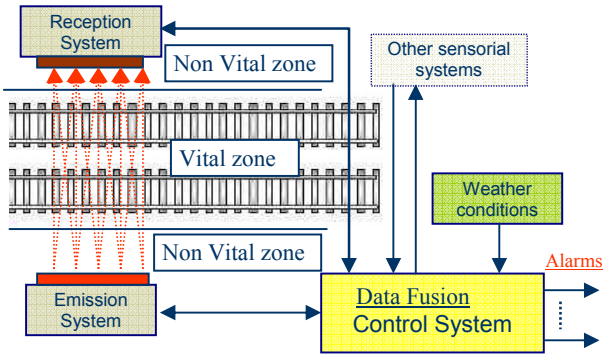

Fig. 1. Infrared barrier, placed in a rail sector.

The topology of the proposed system is similar to one in Figure 1, using three individual emitters in every emitting sensor. In order to detect obstacles in the railway, discriminating at least the vital area (into the rail lines) from the non-vital areas (outside the lines), a special structure has been designed. In this case, every emitter provides three beams (multi-emission): one impacts on the receiver placed

0-7803-9252-3/05/$20.00 ©2005 IEEE

at the axial axis, and the other ones to both sides, as it is shown in Figure 2.

The distance among emitting sensors is 25 cm, in order to detect 0.5x0.5x0.5m objects successfully (size determined by rail regulations) [7]. The configured distance among emitters and receivers is 14 meters in a high-speed line. Basically, the method of obstacle detection, and its location inside the railway, is based on the lack of reception in detectors. For a more detailed discussion, see [8].

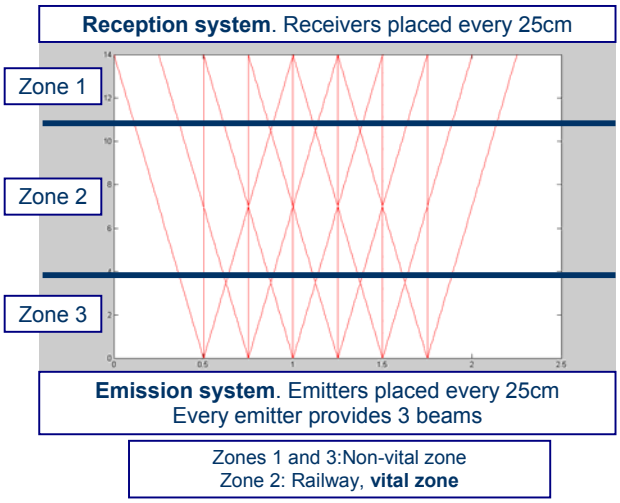

Fig. 2. Infrared barrier with multi-emission.

Obviously, if more emitting transducers were used for every emitting sensor, the position of obstacles could be discriminated with more precision. This aspect, not only makes more expensive the sensorial system, but also does not provide any additional interest to this application, where the main goal is only to determine if there is any on the railways, not considering its accurate position.

This system can be installed both in zones of tunnels or bridges, and in level crossings. In the latter, the infrared barrier can be joined to the crossing gate.

III. EMISSION CODIFICATION

The emission is carried out in a continuous way by the emitters; and when the receivers do not detect this emission, the presence of an obstacle can be concluded. According to the geometry of the system in Figure 2, the radiation coming from three emitters is received by every receiver. In order to be able to discriminate the source of these emissions, it is necessary to code every emission. If interferences among the three codes are not desirable, mutually orthogonal (MO) sets of sequences have to be used.

A. MO sets of sequences

Here, MO sets of sequences are briefly described; for a more detailed discussion, see [9][10].

Let ϕ_{AjAj} denote the autocorrelation function of the binary sequences A_j, and let $\phi_{AjAj}(l)$ denote the *l*-th element in the sequence ϕ_{AjAj}. The binary sequences A_j have two kind of elements {-1,+1}. A set of sequences (A_j, $1 \le j \le M$) is a complementary set of sequences of length *L* if it meets (1).

$$\sum_{j=1}^{M} \phi_{AjAj}(l) = \begin{cases} M \cdot L & if \quad j = 0 \\ 0 \quad \forall \quad j \neq 0 \end{cases} \qquad (1)$$

Let ϕ_{AjBj} denote the cross-correlation function of the sequences A_j and B_j, and let $\phi_{AjBj}(l)$ denote the *l*-th element in the sequence ϕ_{AjBj}. The sets of sequences (B_j, $1 \le j \le M$) and (A_j, $1 \le j \le M$) are mutually orthogonal if:

1. The length of A_j is equal to the length of B_j, for $1 \le j \le M$. In this case, *L* denotes the length of the sequences.
2. Both sets are complementary sets.
3. Equation (2) is met.

$$\sum_{j=1}^{M} \phi_{AjBj}(l) = 0 \quad \forall l \qquad (2)$$

B. Codification

Keeping in mind that at least three orthogonal sets of sequences are required (one per every received signal in the receiver), the minimum dimension of the set should be 3. Nevertheless, since this is not feasible, a set of 4 sequences is used. In this way the whole analysis will be carried out by supposing 4 sequences per set, but only 3 will be used in the real system. So, if *M=4*, and every sequence in the set is denoted {a,b,c,d} then:

$$\begin{aligned} &\phi_{aa}(n) + \phi_{bb}(n) + \phi_{cc}(n) + \phi_{dd}(n) = 4L, \text{ if n = 0} \\ &\phi_{aa}(n) + \phi_{bb}(n) + \phi_{cc}(n) + \phi_{dd}(n) = 0, \text{otherwise} \end{aligned} \qquad (3)$$

The set used in the emitter, not only discriminates the source of the emission, but also provides a high noise immunity to the system, as the obtained results show. The generation of the set is carried out from a seed W [11]. The seeds should meet the relation shown in Table I, in order to obtain the MO sets.

TABLE I.
SEEDS FOR OBTAINING THE ORTHOGONAL SETS.

Set of length L	Seed
Set 1={a_1,b_1,c_1,d_1}	W
Set 2={a_2,b_2,c_2,d_2}	W+L/4
Set 3={a_3,b_3,c_3,d_3}	W+2*L/4
Set 4={a_4,b_4,c_4,d_4}	W+3*L/4

Figure 3 shows the mentioned situation, but with four emitters and one receiver. The emitter and receiver units are synchronized, mainly because of safety reasons in the described application.

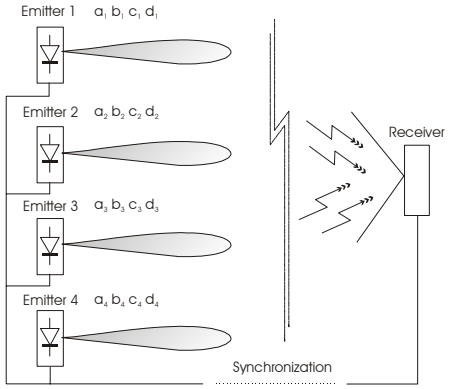

Fig. 3. Detail of the four emitters and the receiver.

In Figure 3, every emitter i transmits the set $\{a_i, b_i, c_i, d_i\}$ continuously. Its continuous emission allows a signal to be obtained in the detector with period L with a maximum peak of $4 \bullet L$, showing that there is not an obstacle between the emitter and the receiver, according to (4). The index i means any emission in the system, $i=\{1, 2, 3, 4\}$.

$$Detector\_output_i = 4L \sum_{k=-\infty}^{k=\infty} \delta(n - k \cdot L) \qquad (3)$$

Figure 4 shows the results when using 64-bit sequences, with a SNR of -12 dB. In Figure 4 there is only one emission, and the detection has been carried out.

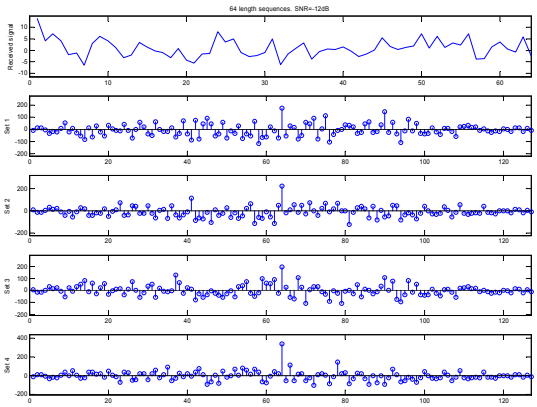

Fig. 4. Detector output for every emission. (L=64, SNR=-12dB).

The outputs are periodic signals, and the period depends on the sequence length. In this system, using 256-bit sequences, a peak is obtained in the detectors every 5.12 ms without any obstacle. The peak detector threshold is fixed to $2 \bullet L=512$. The correlation system (see Figure 7) has been implemented in a FPGA, and Figure 5 shows the real detection without obstacles. If an obstacle is detected in front of a receiver, the shown peaks in Figure 5 disappear, being the output null while the obstacle is in the railway.

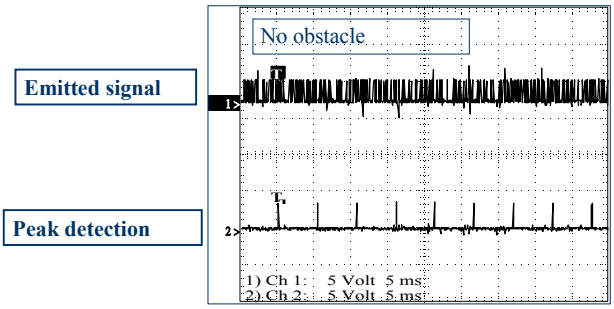

Fig. 5. Real detection every 5.12 ms without obstacles.

C. Application to the infrared emission

Taking into account that the maximum efficiency of the infrared emitters is achieved for pulsed emissions, in order to carry out the emission of both symbols {-1,+1}, a pulse position modulation has been used. In Figure 6, the code assignment is shown, considering that the symbol duration is T seconds. In [12] the process of sequence detection is described in detail.

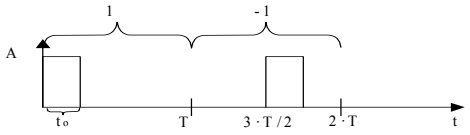

Fig. 6. Pulsed excitation for an IRED and code assignment.

IV. FALSE ALARMS DISCRIMINATION

The outdoor infrared emission suffers from diverse losses, which can produce a wrong detection in the receiver. If the receiver does not detect one emission during a predefined time, an alarm will be generated, informing that there is an obstacle. But if the obstacle does not exist, the alarm is actually false. As far as possible, it is necessary to avoid the false alarms generation, so, they have to be discriminated.

A. False alarms generation

In these outdoor optical systems there are some phenomena that can provide false alarms, mainly the weather conditions and the solar radiation. There are other reasons, as propagation losses or wrong alignment among emitters and receivers. We assume that the last ones have been already considered in the link design.

1. Atmospheric attenuation. Snow, fog and rain are considered. Although there are numerous studies about the losses due to the meteorology, the expression (4) is widely used to quantify them [13].

$$L_{atm}(dB) = \frac{17}{V}\left(\frac{\lambda}{550}\right)^{-q} \cdot R \qquad (4)$$

where
V is the visibility in kilometers;
λ, the wavelength in nanometers;
R, the link range in kilometers;
q, the size distribution of the scattering particles, related to the visibility, which takes the values indicated in the Table II.

TABLE II
RELATION BETWEEN VISIBILITY AND q

Visibility V	**Weather condition**	**q**
V>50km	Very clear	1.6
6km<V<50km	Clear	1.3
1km<V<6km	Haze /snow /light rain	$0.585 \cdot V^{1/3}$
0.5km<V<1km	Light fog /snow / heavy rain	$0.585 \cdot V^{1/3}$
V<0.5km	Thick fog	$0.585 \cdot V^{1/3}$

If this attenuation is very strong, the correlation level can not be high enough, and the system can consider that an obstacle exists.

2. Solar interference. As the photodiode wavelength (850nm) is inside the solar spectrum, natural background light can potentially interfere with signal reception. In some circumstances, direct sunlight may cause link outages for periods of several minutes when the sun is within the receiver's field of view [14]. However, the times, when the receiver is most susceptible to the effects of direct solar radiation (either at dawn or at dusk), can be easily estimated. There are some solutions to mitigate this problem, like proper orientation or use of a narrow-bandwidth light filters, but it is almost impossible to avoid them completely. It is important to remember that interference by reflected sunlight is possible as well. The solar effect in the IR barrier is the photodiode saturation. It implies that the sequence detection does not work, providing a lack of reception as if there was an obstacle.

B. False alarms discrimination

When there are neither obstacles in the railway nor false alarms, the correlator outputs are shown in Figure 5.

In this situation, when there is a lack of signal due to the weather conditions or solar interference, false alarms can be produced. To avoid it, we propose the use of a dynamic threshold for the peak detector. Every correlator output, $y_j[k]$, is estimated by polynomial interpolation of degree 1, and the estimated output, $\hat{y}_j[k]$, is used to change periodically the threshold. The polynomy computes with N-samples windows, and the threshold is determined to the half of the first estimated output in a window. Figure 7 shows the block diagram of the system for 4 emitters and one receiver, with the periodical threshold correction. The reception block is the same for every receiver, but changing the codification set.

The algorithm has been simulated in different weather conditions with a SNR=0dB. In Figure 8, the first graph shows the correlator output for different weather conditions, the estimated output and the dynamic threshold. The graph at the bottom shows the peak detector output using a fixed threshold. It can be observed that with thick fog, there are some errors in the obstacle detection. The central graph shows the peak detector output, but now using the dynamic threshold, and the obstacle detection is correct. Figure 9 shows the same situation, but the interpolation error, $\hat{y}_j[k] - y_j[k]$, has been represented at the bottom. This error can be used to validate the peak detector output. We can conclude that in these conditions, the polynomial interpolation reduces the false alarms due to the atmospheric attenuation.

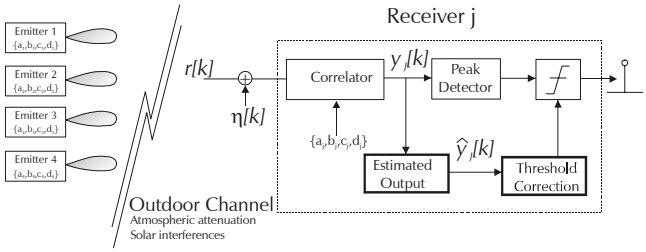

Fig. 7. Block diagram of the system with dynamic threshold.

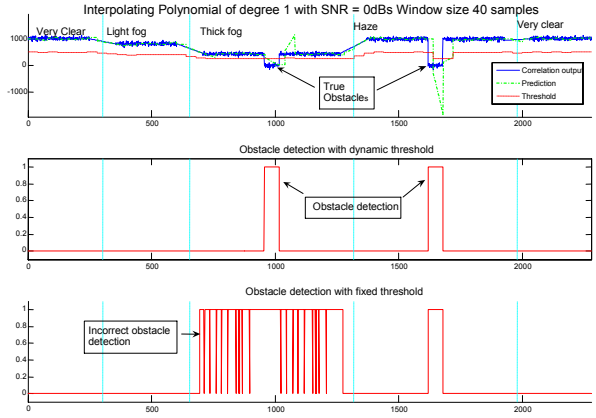

Fig. 8. Dynamic threshold evaluation in different weather conditions.

Figure 10 shows the simulation with different relative levels of sunlight, increasing with the time, and with SNR=0dB. The black spot represents an obstacle. The higher is the solar radiation, the lower is the correlator output. In this situation, the dynamic threshold works better than the fixed one. There are only errors when the sun interference is too high, compared to the emitted signal (the emitted signal has been normalized to one).

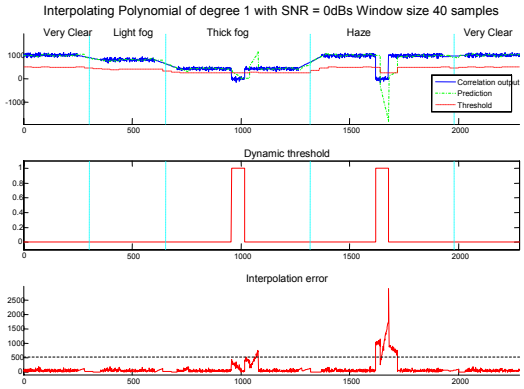

Fig. 9. Interpolation error.

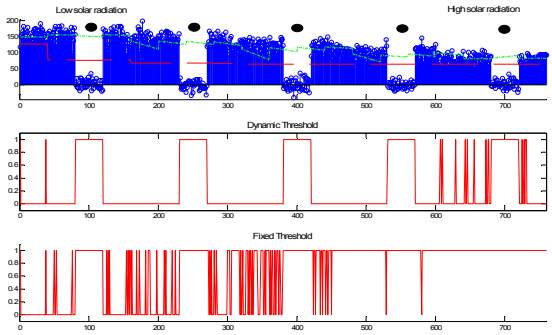

Fig. 10. Dynamic threshold evaluation with different relative levels of sunlight.

V. OBSTACLE LOCATION

Once the existence of an obstacle has been detected in the railway with high reliability, it is possible to locate it by taking advantage of the geometrical distribution of the sensors.

The location algorithm obtains the longitudinal and transverse position. To obtain the longitudinal one, it only is necessary to know the lack of reception in the axial axis, between emitter and receiver (see Figure 2). The detection area has been divided into three transverse zones, as figure 11 shows.

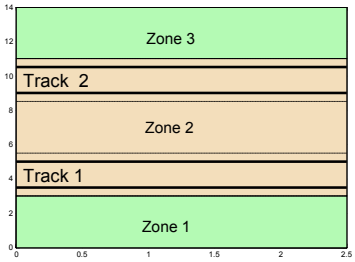

Fig. 11. Transverse zones.

Taking into account that the peak detector output is zero {0} if there is an obstacle, and one {1} if not, the location algorithm can be regarded as a Boolean one. There are three Boolean functions, one for every zone. These functions are based on the lowest number of beams that can locate the minimum obstacle (50x50x50 cm) in the three zones. This group of beams can be repeated along the track to develop the infrared barrier. Figure 12 shows the chosen beams. Eight emitters and four receivers are considered.

Every receiver has three bits (one for every detected emission). Let [R_{i1}, R_{i2}, R_{i3}] denote the three bits of the receiver i (i =1, 2, 3 and 4), the Boolean functions that determine the presence of obstacle in a zone are (5)-(7).

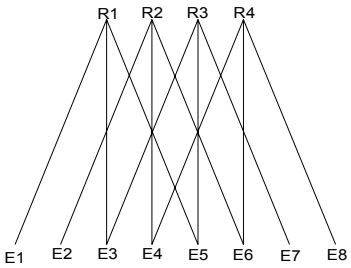

Fig. 12. Minimum number of sensors to obtain transverse position.

$$zone_1 = \overline{R_{12}} \cdot R_{13} \cdot \overline{R_{22}} \cdot \overline{R_{31}} \cdot R_{32} \cdot \overline{R_{41}} \cdot R_{42} + \\ + R_{12} \cdot \overline{R_{13}} \cdot R_{22} \cdot \overline{R_{23}} \cdot \overline{R_{32}} \cdot R_{41} \cdot \overline{R_{42}} \quad (5)$$

$$zone_2 = \overline{R_{12}} \cdot \overline{R_{13}} \cdot R_{21} \cdot \overline{R_{22}} \cdot \overline{R_{31}} \cdot R_{32} \cdot R_{41} \cdot R_{42} + \\ + R_{12} \cdot R_{13} \cdot R_{22} \cdot \overline{R_{23}} \cdot \overline{R_{32}} \cdot R_{33} \cdot \overline{R_{41}} \cdot R_{42} + \\ + \overline{R_{12}} \cdot \overline{R_{13}} \cdot \overline{R_{21}} \cdot \overline{R_{22}} \cdot R_{23} \cdot \overline{R_{31}} \cdot R_{32} \cdot R_{41} \cdot R_{42} + \\ + R_{12} \cdot R_{13} \cdot R_{22} \cdot \overline{R_{23}} \cdot R_{31} \cdot \overline{R_{32}} \cdot R_{33} \cdot \overline{R_{41}} \cdot \overline{R_{42}} \quad (6)$$

$$zone_3 = \overline{R_{12}} \cdot \overline{R_{13}} \cdot \overline{R_{21}} \cdot \overline{R_{22}} \cdot \overline{R_{23}} \cdot R_{31} \cdot R_{32} \cdot R_{42} + \\ + R_{12} \cdot R_{13} \cdot \overline{R_{21}} \cdot \overline{R_{22}} \cdot \overline{R_{23}} \cdot \overline{R_{31}} \cdot \overline{R_{32}} \cdot R_{42} + \\ + R_{12} \cdot \overline{R_{22}} \cdot \overline{R_{23}} \cdot \overline{R_{31}} \cdot \overline{R_{32}} \cdot \overline{R_{33}} \cdot R_{41} \cdot R_{42} + \\ + R_{12} \cdot R_{22} \cdot R_{23} \cdot \overline{R_{31}} \cdot \overline{R_{32}} \cdot \overline{R_{33}} \cdot R_{41} \cdot R_{42} + \\ + \overline{R_{12}} \cdot \overline{R_{13}} \cdot \overline{R_{21}} \cdot \overline{R_{22}} \cdot \overline{R_{23}} \cdot \overline{R_{31}} \cdot \overline{R_{32}} \cdot \overline{R_{33}} \cdot R_{41} \cdot R_{42} + \\ + R_{12} \cdot R_{13} \cdot \overline{R_{21}} \cdot \overline{R_{22}} \cdot \overline{R_{23}} \cdot \overline{R_{31}} \cdot \overline{R_{32}} \cdot \overline{R_{33}} \cdot \overline{R_{41}} \cdot \overline{R_{42}} \quad (7)$$

This algorithm has been simulated with fixed and mobile obstacles. Figure 13a represents a passing train in one of the tracks, and Figure 13b shows a pedestrian crossing the tracks. In this second figure only one position of the pedestrian has been represented. If the object is bigger than 0.5m, six beams are not received, so other current systems are improved since only two beams are not received for them. In both figures, the remarked area shows the possible obstacle location, according to its dimensions and the non-received beams.

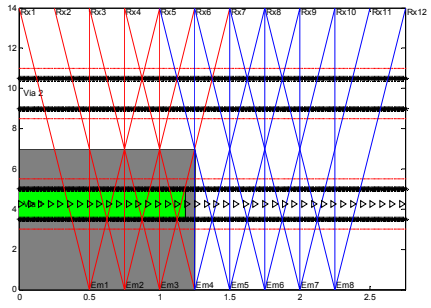

(a)

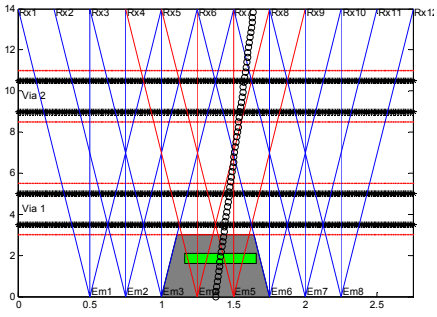

(b)

Fig. 13. Obstacle detection and location in the railway.

VI. CONCLUSIONS

A proposal of a system for obstacle detection in railways has been carried out. Its geometry allows, not only to detect the presence of obstacles, but also to locate them inside the analysis region, discriminating between a vital area and a non-vital one.

In any situation, if the obstacle is bigger than 0.5 m, at least 6 beams are not received, being the system highly redundant. This is an added worth if the barrier is compared to traditional ones.

The codification technique based on MO sets of sequences provides a high immunity against the infrared channel degradation. A prototype has been designed to test the feasibility of the codification.

Typical false alarms have been analyzed, and a first solution has been presented to avoid them. The interpolation algorithm permits to choose a proper threshold taking into account the degradation of the channel. Other algorithms, as the Kalman filter, should be tested.

Though simulations show the feasibility of the proposed solutions, a new prototype is being implemented to perform real outdoor tests, using the interpolation algorithm.

VII. ACKNOWLEDGMENT

The work described in this paper has been possible by funding from the Ministry of Science and Technology - Projects SILPAR (reference DPI2003-5067) and PARMEI (reference DIP2003-08715-C02-01)- and the University of Alcalá through the ISUAP project (ref. PI2004/033).

VIII. REFERENCES

[1] http://www.laseroptronix.com/rail/

[2] http://www.smartmicro.de/computer_vision.html

[3] Ota, Masaru "Obstacle Detection System with Stereo Cameras for Level Crossings", *Railway Technology Avalanche*, No.5, March 1, 2004.

[4] http://spt.dibe.unige.it/ISIP/Projects/pft3.html

[5] S. Lohmeier, R. Rajaraman, V. Ramasami. "Development of an Ultra-Wideband Radar System for Vehicle Detection at Railway Crossings". 0-7803-7537-8/02 *IEEE*, 2002.

[6] G.L. Foresti et al, "Progressive Image Coding for Visual Surveillance Applications based on Statistical Morphological Skeleton". *8th International Conference on Signal Processing, EUSIPCO96*, Trieste, Italy, September 12-15, 1996.

[7] "Sistema de detección de caída de obstáculos a vía. Requisitos técnicos y funcionales". GIF. 2001

[8] J.Jesús García, Jesús Ureña, Álvaro Hernández, Manuel Mazo, J.Carlos García, Fernando Álvarez, J. Antonio Jiménez, Patricio Donato, Carmen Pérez."IR sensor array configuration and signal processing for detecting obstacles in railways" *Third IEEE Sensor Array and Multichannel Signal Processing Workshop SAM'04*.

[9] Tseng, C.-C. and Liu, C.L.: "Complementary Sets of Sequences", *IEEE Trans. Inform. Theory*, vol. IT-18, No. 5, Sep. 1972, pp. 644-652.

[10] Shu-Ming Tseng; Bell, M.R.; "Asynchronous multicarrier DS-CDMA using mutually orthogonal complementary sets of sequences", *IEEE Transactions on Communications Volume 48*, Issue 1, Jan. 2000 Page(s):53 – 59

[11] Fernando J. Álvarez, Jesús Ureña, Manuel Mazo, Álvaro Hernández, Juan J. García, José A. Jiménez y Patricio G. Donato. "Nuevo Algoritmo para la Generación Eficiente de Conjuntos de Cuatro Secuencias Complementarias" *TELEC'04 International Conference. Telecommunications, Electronics and Control*.

[12] J. Ureña, J.J. García, M. Mazo, Á. Hernández, J.C. García, -R. García. "Mejora en la detección con sensores de infrarrojos mediante la codificación de la emisión". *SAAEI'2003*. Vigo, España, Septiembre 2003.

[13] Isaac I. Kim, Ron Stieger, Joseph A. Koontz, Carter Moursund, Micah Barclay, Prasanna Adhikari, John Schuster, Eric Korevaar, Richard Ruigrok, Casimer DeCusatis "Wireless optical transmission of fast ethernet, FDDI, ATM, and ESCON protocol data using the TerraLink laser communication system", *Optical Engineering*, Vol. 37 No. 12, December 1998

[14] Scott Bloom, AirFiber; Eric Korevaar, MRV Communications; John Schuster, Terabeam; Heinz Willebrand, LightPointe Communications, "Understanding the performance of free-space optics [Invited]" *Journal of Optical Networking*, June 2003, Vol 2 nº 6, pp 178-200